Available online at www.sciencedirect.com
SCIENCE DIRECT
International Journal of Pharmaceutics 313 (2006) 23–28
INTERNATIONAL JOURNAL OF PHARMACEUTICS
www.elsevier.com/locate/ijpharm

Investigating the moisture-induced crystallization kinetics of spray-dried lactose

D.J. Burnett [a,*], F. Thielmann [b], T. Sokoloski [c], J. Brum [c]

[a] *Surface Measurement Systems Ltd., 2222 South 12th Street, Suite D, Allentown, PA 18103, USA*
[b] *Surface Measurement Systems Ltd., 5 Wharfside, Rosemont Road, Alperton, Middlesex HA0 4PE, UK*
[c] *GlaxoSmithKline, 1250 South Collegeville Road, Collegeville, PA 19426, USA*

Received 16 August 2005; received in revised form 6 January 2006; accepted 10 January 2006
Available online 8 February 2006

Abstract

Gravimetric water sorption experiments were performed to study the crystallization behavior of amorphous spray-dried lactose over a wide range of temperature and humidity conditions. Experiments performed at 25 °C between 48 and 60% relative humidity (RH) showed that the onset time to crystallization increased dramatically with decreasing humidity. At 55% RH and above, crystallization occurred in a single detectible step, while below a two-step process was observed. Experiments performed at 51% RH between 22 and 32 °C indicated the induction time to crystallization onset increased with decreasing temperature. Above 25 °C at 51% RH, crystallization occurred in one measurable step, while below crystallization occurred in two steps. The constant RH with varying temperature results were modeled to determine the crystallization mechanism. Above 25 °C a mechanism consisting of two competing reaction sequences fit the data with a 0.9997 correlation coefficient. Both reaction sequences have two steps: an auto-catalytic first step is followed by a three-dimensional diffusion controlled water loss step.

Keywords: Vapor sorption; Phase transition; Humidity; Amorphous; Crystallization kinetics; Spray-drying

1. Introduction

Amorphous materials have an increasing importance in the pharmaceutical industry. The presence of amorphous phases in pharmaceutical formulations can generally be attributed to one of three circumstances: (1) the material may be deliberately manufactured in an amorphous state; (2) the material may be inherently amorphous or partially amorphous at processing or delivery conditions; or (3) the amorphous material may be produced unintentionally through milling, compression, or introduction of impurities (Craig et al., 1999). The presence of amorphous materials in pharmaceutical formulations can dramatically affect the processing, storage, bioavailability, and delivery properties of these materials.

Numerous low molecular weight amorphous materials will revert to their more thermodynamically stable, crystalline forms if exposed to conditions above the glass transition. Crystallization rates can be affected by temperature (Vney et al., 1995; Kedward et al., 1998; Takeuchi et al., 1999), relative humidity (Jouppila et al., 1998; Kedward et al., 2000a; Burnett et al., 2004), and other neighboring materials (Iglesias and Chirafe, 1978; Arvanitoyannis and Blanshard, 1994; Imamura et al., 1998; Tzannis and Prestrelski, 1999). In particular, water vapor can have a dramatic effect on amorphous materials. Amorphous solids often absorb relatively large amounts of water vapor compared to their corresponding crystalline phases. Sorbed water can act as a plasticizing agent, thus significantly lowering the glass transition temperature below the storage temperature and cause phase transitions and lyophile collapse (Roos and Karel, 1991). Additionally, moisture sorption can lead to particle agglomeration and powder caking.

Spray-dried lactose is commonly used in solid formulations and is likely to be the most commonly used (partially) amorphous material in the pharmaceutical industry (Schmitt et al., 1999). Additionally, there is an abundance of information regarding its crystallization and polymorphic forms (Wade and Weller, 1994). The degree of lactose crystallinity can affect tabletting properties (Huettenrauch, 1978; Sebhatu

* Corresponding author. Tel.: +1 610 798 8299; fax: +1 610 798 0334.
E-mail address: burnett@smsna.com (D.J. Burnett).

0378-5173/$ – see front matter © 2006 Elsevier B.V. All rights reserved.
doi:10.1016/j.ijpharm.2006.01.012

and Alderborn, 1999), storage of micronized powders (Bystron and Briggner, 1994), texture (Kedward et al., 2000a), and flow properties (Lai and Schmidt, 1990). Therefore, understanding the crystallization behavior of amorphous lactose is vital for the successful development, processing, and storage of formulations containing amorphous lactose. This contribution investigates the crystallization kinetics and mechanism over a range of temperatures and humidities.

Due to the use of amorphous lactose in pharmaceutical formulations, its crystallization behavior has been studied extensively using a variety of techniques including differential scanning calorimetry (DSC) (Roos and Karel, 1991; Arvanitoyannis and Blanshard, 1994; Kedward et al., 1998, 2000a; Schmitt et al., 1999), X-ray diffraction (XRD) (Jouppila et al., 1998; Haque and Roos, 2005), gravimetric vapor sorption (Schmitt et al., 1999), atomic force microscopy (AFM) (Mahlin et al., 2004), and polarized light microscopy (Mazzobre et al., 2003). Several theories have been applied to model the lactose crystallization mechanism. For instance, the Avrami equation or similar derivatives have been used by several researchers (Arvanitoyannis and Blanshard, 1994; Jouppila et al., 1998; Schmitt et al., 1999; Kedward et al., 2000a,b; Mazzobre et al., 2003; Haque and Roos, 2005). According to the original Avrami theory, the n factor gives an indication on the crystallization mechanism. However, in recent years it has been customary to regard this as an adjustable factor. Other empirical kinetic models have been applied to lactose crystallization including: the Ahrrenius equation, the Williams, Landel, and Ferry (WLF) equation, and the Hoffman equation (Arvanitoyannis and Blanshard, 1994). Despite the successful application of the above models, the fundamental mechanistic information derived from these equations is limited. This aim of this paper is to understand the moisture-induced crystallization of lactose on a fundamental, mechanistic basis without assuming any previously derived crystallization models.

Above the glass transition, many low molecular weight amorphous materials will relax to their more stable, crystalline state. The amorphous material will typically have a greater water vapor sorption capacity than the crystalline material, due to increased void space, free energy, and/or surface area. This can be measured directly using gravimetric techniques and has been used previously to determine amorphous contents below one percent (Saleki-Gerhardt et al., 1994; Buckton and Darcy, 1995; Mackin et al., 2002). When the material undergoes an amorphous to crystalline transition, the water sorption capacity will typically decrease drastically. This results in an overall mass loss as excess water is desorbed during crystallization. Therefore, this mass loss can be used to monitor an amorphous to crystalline transition.

2. Materials and methods

Gravimetric vapor sorption experiments have been carried out using the DVS-1 instrument (Surface Measurement Systems, London, UK). This instrument measures the uptake and loss of vapor gravimetrically using a recording ultra-microbalance with a mass resolution of ±0.1 μg. The vapor partial pressure (±1.0%) around the sample is controlled by mixing saturated and dry carrier gas streams using electronic mass flow controllers. The desired temperature is maintained at ±0.1 °C.

The samples (~25 mg) were placed into the DVS-1 instrument at the desired temperature where they were initially dried in a 200-standard cubic centimeters (sccm) stream of dry air (<0.1% relative humidity) for several hours to establish a dry mass. The samples were then exposed to a step change in relative humidity (RH) and maintained at these conditions while monitoring the sample mass. The mass will initially increase as the sample sorbs water. The derivative of the mass versus time plots were performed and the onset time for crystallization was taken as the point where the derivate intercepts the x-axis (i.e. slope of mass versus time turns negative). The humidity was maintained at the desired level until crystallization was complete. Crystallinity of the end material was verified by exposing the sample to 95% RH. Absence of the mass loss feature at high relative humidity values was taken as an indication of complete crystallinity of the end material.

Amorphous lactose was prepared by GlaxoSmithKline (Collegeville, PA, USA) by dissolving crystalline lactose in water (10%, w/w) and spray-drying at 190 °C. No further processing, screening, or characterization was performed on the spray-dried lactose. The spray-dried lactose was stored over desiccant (anhydrous calcium sulfate) at 6 °C, to limit any premature crystallization. The same batch of spray-dried lactose was used for these studies to minimize any particle size, surface area, impurity, or similar batch-to-batch effects.

The modeling of the crystallization data was done using the routines found in NETZSCH Thermokinetics® software. This software allows for visual/manual manipulation of fit parameters and then performs the least squares optimization itself to generate the best-fit parameters. Initial model selection is experience based as well as based on observation of the consequence of effects visually seen upon manual parameter manipulation.

3. Results and discussion

3.1. Gravimetric data

A typical moisture-induced crystallization result is displayed in Fig. 1 for amorphous lactose at 25.0 °C. The solid line traces the percentage change in mass (referenced from the dry mass)

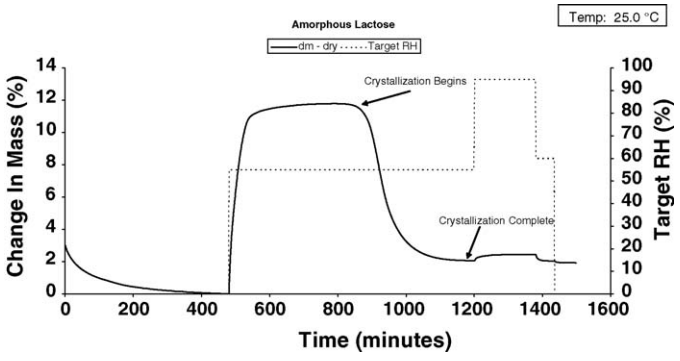

Fig. 1. Amorphous lactose crystallization at 55% RH and 25 °C.

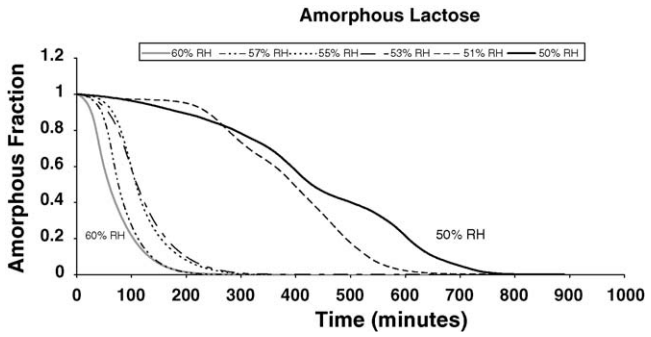

Fig. 2. Amorphous fraction as a function of time between 50 and 60% RH at 25 °C.

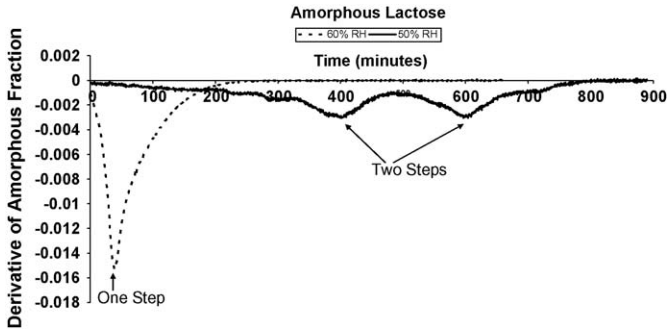

Fig. 3. Derivative of amorphous fraction as a function of time at 50 and 60% RH at 25 °C.

on the left *y*-axis as a function of time. The dashed line follows the target relative humidity on the right *y*-axis as a function of time. During the drying period, the sample mass decreases by approximately 3%. As the humidity is rapidly increased to 55% RH, the sample mass increases dramatically due to water vapor sorption. After a period of time, the sample mass begins to steadily decrease. This characteristic mass loss feature has been well documented and has been previously assigned to the crystallization of amorphous lactose (Buckton and Darcy, 1995; Burnett et al., 2004; Price and Young, 2004). The lag between the increase in humidity and the point where mass loss is observed is taken as the onset time for crystallization. This point was determined by plotting the derivative of the mass versus time and identifying the *x*-intercept (i.e. where the mass versus time slope becomes negative). After crystallization is complete, the mass loss slows and approaches an equilibrium value. As the humidity is then increased to 95% RH, the sample mass increases and rapidly approaches equilibrium. The absence of any mass loss during this step confirms the sample is completely crystalline. The slight mass increase observed during this step is due to surface water adsorption on the fully crystallized lactose.

In our previous work (Burnett et al., 2004), it was determined that water vapor induces a glass transition at 30% RH and a crystallization event at 58% RH for spray-dried lactose at 25 °C. Below 30% RH, no crystallization was observed over the time scale of the experiments (1 week) and above 58% RH crystallization was nearly instantaneous. Therefore, experiments have been performed on amorphous lactose at 25.0 °C over a range of relative humidities between the glass transition and crystallization humidity points. Over this regime, crystallization will be kinetically controlled. Fig. 2 displays the moisture-induced crystallization results for amorphous lactose between 50 and 60% RH. The time has been normalized such that the onset point of crystallization has been shifted to a time of zero. The *y*-axis has been normalized to reflect the amorphous fraction. Before crystallization, the amorphous fraction is assumed to be one and after crystallization the amorphous fraction is set to zero. The gravimetric results in Fig. 2 indicate a one-step crystallization process at 53, 55, 57, and 60% RH. For these experiments, the amorphous fraction decreases precipitously in one step. However, at 51 and 50% RH, there is an initial decrease, followed by a 'leveling off' in the amorphous fraction. This is followed by a second decrease, resulting in an apparent two-step crystallization mechanism at these conditions. This is highlighted in Fig. 3 where the derivative of the amorphous fraction is plotted versus time for the results at 60% RH (dashed line) and 50% RH (solid line). Clearly, a single peak is observed at 60% RH indicating a one-step mechanism, while two peaks are evident at 50% RH, illustrating a two-step mechanism.

The onset times for crystallization at 25 °C between 48 and 60% RH are displayed in Fig. 4. These values were taken as the *x*-intercept from derivative of mass versus time plots (i.e. change in mass becomes negative). As the humidity is increased, the onset time for crystallization decreases. As the humidity is increased, the amorphous lactose sample will sorb more water, thus facilitating plasticization and lyophile collapse. Previous researchers have observed similar lactose crystallization trends with relative humidity (Haque and Roos, 2005). An exponential fit was applied to the data as shown by the solid line in Fig. 4. There is only general agreement between the data and the exponential fit. More sophisticated modeling will be discussed below.

Additional experiments at a constant RH over a range of temperatures were performed to probe the effects of temperature on the crystallization behavior of amorphous lactose. Fig. 5 displays a series of experiments at 51% RH between 22 and 32 °C. Similar to Fig. 2, these results show the amorphous fraction versus time. Again, the time scale is normalized such that the onset time for crystallization is taken as the zero point. For the experiments above 25 °C the amorphous fraction decreases sharply in one step, but at 25 °C and below the lactose appears to crystallize in two distinguishable steps. These results are similar to the

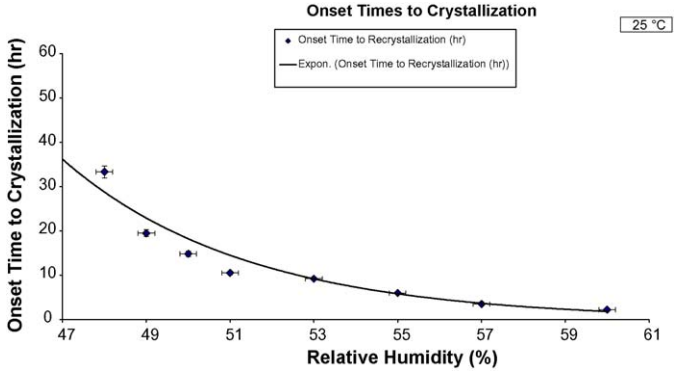

Fig. 4. Onset times for crystallization as a function of relative humidity at 25 °C.

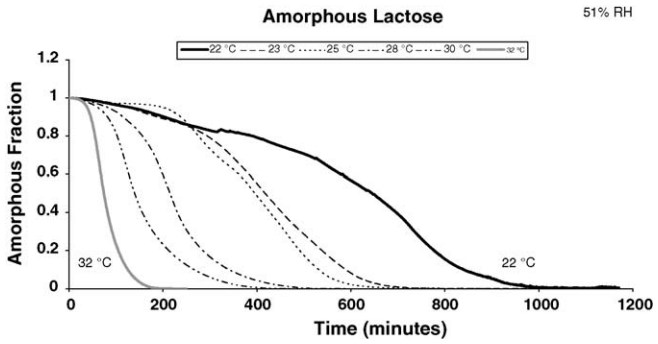

Fig. 5. Amorphous fraction as a function of time between 22 and 32 °C at 51% RH.

results at 25 °C over a range of humidities (see Fig. 2). At high humidities and high temperatures only one crystallization step is visible in the gravimetric data, but at low humidities and low temperatures evidence of two steps is visible. Derivative plots (data not shown) were performed for the data in Fig. 5. As in Fig. 3, there are two distinct peaks for the results at 25 °C and below (two-step mechanism), while only one peak is observed above 25 °C (one-step mechanism). It is quite possible that the same two reaction steps are present over all conditions studied, but only visible in the gravimetric data when the crystallization kinetics are significantly slowed down by low temperature or low humidity conditions.

The onset times for crystallization at 51% RH over a range of temperatures are displayed graphically in Fig. 6. Again, these onset times are obtained from the *x*-intercept of mass derivative versus time plots, as discussed previously. As the temperature is increased, the induction time to crystallization decreases rapidly. Similar results have been obtained previously using DSC, PLV, and gravimetric methods (Roos and Karel, 1991; Arvanitoyannis and Blanshard, 1994; Schmitt et al., 1999; Mazzobre et al., 2003). These results are expected since viscosity decreases considerably as temperature increases. The increased molecular motion facilitates sample crystallization. In this study there appears to be a strong relationship between the crystallization induction time and temperature at 51% RH. An exponential equation has been fit to the data (solid line in Fig. 6) indicating only a general agreement with the data. An exponential relationship between crystallization induction times and temperature was observed for lactose crystallization using DSC and PLV

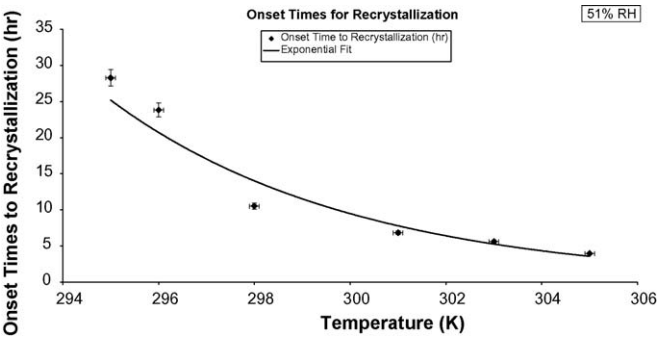

Fig. 6. Onset times for crystallization as a function of temperature at 51% RH.

(Mazzobre et al., 2003), but this study only weakly supports an exponential relationship.

The data in Fig. 6 was fit to an Arrhenius plot in order to obtain an apparent activation energy. The reciprocal of the induction time was taken as the rate; therefore the activation energy obtained would only be for the initial reaction step. Using the data in Fig. 6, an apparent initial activation energy of 146 kJ/mol was obtained. Activation energies of 112 and 104 kJ/mol were obtained using similar gravimetric techniques at 57.5% RH between 18 and 32 °C (Schmitt et al., 1999). The value obtained in this report at 51% RH is higher than the values obtained by other researchers at 57.5% RH. As Figs. 2 and 4 clearly show, crystallization occurs faster at higher relative humidities when measured at the same temperature. Therefore, higher apparent activation energies would be expected at lower humidity conditions, which is consistent with the current results.

3.2. Crystallization mechanism modeling

The modeling of the crystallization data was done in the following manner. The first step in the analysis of data is to generate a model-free activation energy as a function of extent of reaction. Three such iso conversion methods have been developed: Friedman Analysis (Friedman, 1965), Ozawa–Flynn–Wall Analysis, and ASTM E698. Of particular importance in these methods is the ability to specify activation energy without having to specify a model. Experience has shown that the Friedman Analysis yields more information. Friedman Energy Plots as well as the others can be generated using the routines found in NETZSCH Thermokinetics® software.

Weaknesses in kinetic analysis of single-curve data have led to the increased acceptance of the use of a multi-curve approach (Opfermann, 2000). A series of isothermal experiments at different temperatures (Isothermal Calorimetry or DVS) or non-isothermal measurements at different heating rates (TGA or DSC) lend themselves to such multiple-curve analysis (multivariate analysis); the behavior of the sample over a global range of the reaction field now is observed. Use is made of data giving the same extent of conversion at different temperatures.

For simple one-step reactions, a single activation energy is obtained as a function of the extent of reaction. It is clear that in a Friedman Analysis for the crystallization of lactose a multi-step reaction is involved. Friedman Analysis gives estimates of activation energies and pre-exponential rate constant terms (assuming first order reaction) which can be used in conjunction with proposed models to best explain the experimental data. An *F*-test is used to decide if one of several models differs significantly from the best model in terms of fit quality. Two variances, S_1 and S_2, are related ($S_2 > S_1$) and compared with the statistical quantile, $F_{crit}(f_1, f_2)$, which is a measure of the confidence level; f_1 and f_2 being degrees of freedom for the two variances.

The results at 51% RH between 22 and 32 °C were used to elucidate the lactose crystallization mechanism. These five data sets were subjected to a Friedman Analysis. The resulting Friedman plot in Fig. 7 shows the activation energy (left *y*-axis; *E*) and pre-exponential factor (right *y*-axis; *A*) versus the fractional mass loss during crystallization. The activation energy is changing

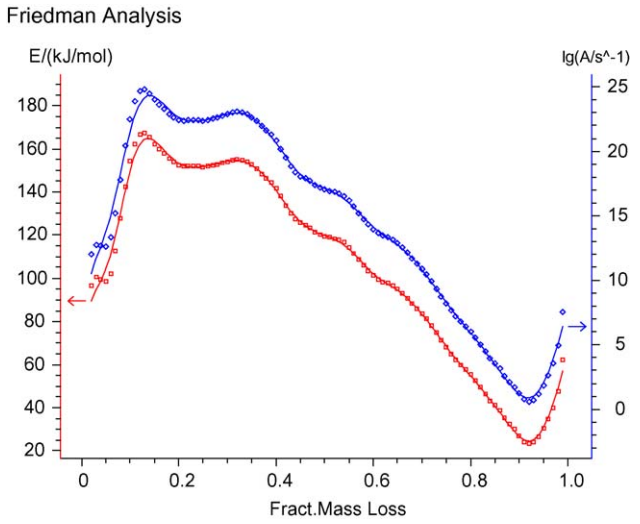

Fig. 7. Friedman plot using the gravimetric crystallization results measured between 22 and 32 °C at 51% RH.

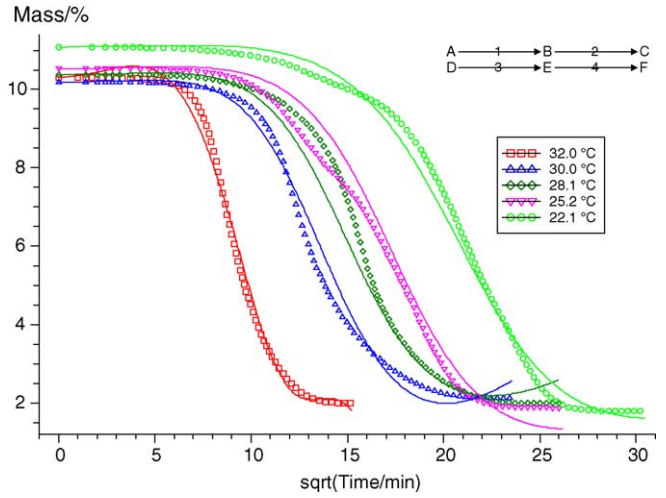

Fig. 9. Gravimetric data between 22 and 32 °C at 51% RH with best-fit mechanism.

significantly throughout the course of the reaction, indicating a multi-step process. If there was a single reaction step, then the activation energy would be constant throughout the entire reaction.

The NETZSCH Thermokinetics® software was used to elucidate the reaction mechanism. The best fit was obtained when using only the data above 25 °C. This coincided with the results where only one step was visible in the gravimetric data. The resulting mechanism and fit is displayed in Fig. 8 for the data at 32.0, 30.0, and 28.1 °C. The correlation coefficient for this mechanism is 0.9997. The mechanism in Fig. 7 indicates two competing, independent reaction sequences. For both reaction sequences, the first step is auto-catalyzed by B and E, respectively. The second step in each reaction sequence is three-dimensionally diffusion limited. The first step in each reaction sequence is most likely crystal nucleation from the amorphous phase, as nucleation would be auto-catalyzed. The initial crystal seeds would propagate, thus creating more crystals. The second step is most likely water diffusing from the bulk of the sample. Amorphous lactose has the ability to absorb water into the bulk

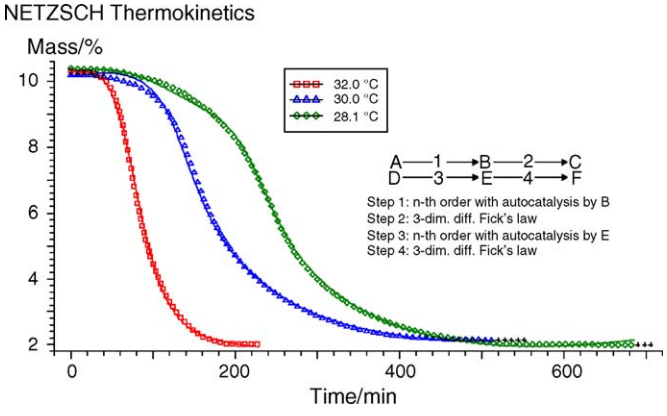

Fig. 8. Gravimetric data above 25 °C at 51% RH with best-fit mechanism.

structure, whereas water sorption would be limited to surface adsorption for crystalline lactose. Therefore, as the amorphous material crystallizes it must desorb water, which would be diffusion limited.

Previous researchers have observed evidence of multiple reaction products during lactose crystallization. For instance, Mitchell et al. observed evidence of a shoulder during the crystallization peak in DSC experiments (Kedward et al., 1998, 2000a). They hypothesized this shoulder was due to crystallization into different forms of lactose. For instance, the lactose may crystallize into the α-monohydrate form and other anhydrous polymorphs (Kedward et al., 1998, 2000a). This hypothesis is given further support by XRD data of amorphous lactose crystallized at different humidity conditions (Jouppila et al., 1998; Haque and Roos, 2005). Amorphous lactose was found to crystallize into the α-lactose monohydrate, anhydrous β-lactose, and the anhydrous forms of α- and β-lactose in molar ratios of 5:3 and 4:1. α-Lactose monohydrate was the predominant species at high humidities, with the anhydrous forms becoming more prevalent at lower humidity conditions (Jouppila et al., 1998). In fact, anhydrous β-lactose was only observed at 44.4% RH, the lowest humidity investigated in the above study. In all, the XRD and DSC results by the above researchers support the multi-reaction sequence obtained by the modeling studies in this report.

When the data at 25 °C and below is considered, the quality of the reaction mechanism fit diminishes. Fig. 9 displays the same reaction mechanism obtained in Fig. 8 applied to all temperatures. When all temperature data are included the correlation coefficient decreases to 0.977. These results are not fully understood at the present time. The lower temperature data exhibit a distinctive shoulder, which is absent in the other higher temperature experiments. There is also a 'shoulder' in the lower humidity data at 25 °C. This 'shoulder' may be due to two reaction sequences with induction times that are affected differently by temperature and humidity. For instance, the first step in one reaction sequence may be more dependent on temperature and/or

humidity than the other reaction sequence. Then, there may be humidity and temperature regimes where the reactions will be concurrent and other regimes where the reaction sequences are independent. Alternatively, a branched reaction may only occur at low temperature and/or humidity conditions. This hypothesis may be supported by the XRD data by Roos and Karel (1991) where anhydrous β-lactose was only observed at the lower humidities. Additional studies over a broader temperature and humidity matrix may help elucidate the nature of this not fully understood feature in the gravimetric data.

4. Conclusions

Amorphous lactose was crystallized over a range of humidity and temperature conditions using a gravimetric sorption apparatus. The induction times for crystallization indicated a strong relationship with both temperature and humidity. Gravimetric experiments and mechanistic modeling indicated a multi-step crystallization process. Crystallization data above 25 °C at 51% RH indicated a mechanism consisting of two competing reaction sequences. The first step of each reaction is auto-catalyzed, while the second step was three-dimensionally diffusion limited. The auto-catalyzed first step is probably due to crystal nucleation, while the second step is most likely water diffusing out of the lactose. The data at low temperature and humidity conditions are not fully understood, but may be due to the formation of multiple conformers of crystalline lactose or reaction sequences with differing induction periods. Additional gravimetric experiments over a broader humidity and temperature matrix combined with methods to determine the crystalline lactose conformations are planned to further understand the low temperature and humidity results.

Acknowledgement

The authors would like to thank Wei Chen of GlaxoSmithKline for providing the spray-dried lactose.

References

Arvanitoyannis, I., Blanshard, J.M.V., 1994. J. Food Sci. 59, 197–205.
Buckton, G., Darcy, P., 1995. Int. J. Pharm. 123, 265–271.
Burnett, D.J., Thielmann, F., Booth, J., 2004. Int. J. Pharm. 287, 123–133.
Bystron, K., Briggner, L.-E., 1994. Respiratory Drug Delivery IV. Virginia Commonwealth University, Richmond, VA.
Craig, D.Q.M., Royall, P.G., Kett, V.L., Hopton, M.L., 1999. Int. J. Pharm. 179, 179–207.
Friedman, H.L., 1965. J. Polym. Sci.: Part C, 183–195.
Haque, M.K., Roos, Y.H., 2005. Carbohydr. Res. 340, 293–301.
Huettenrauch, R., 1978. Acta Pharm. Technol. 6, 55–127.
Iglesias, H.A., Chirafe, J., 1978. J. Food Technol. 13, 137–144.
Imamura, K., Suzuki, T., Kirii, S., Tatsumichi, T., Okazaki, M., 1998. J. Chem. Eng. Jpn. 31, 325–329.
Jouppila, K., Kansikas, J., Roos, Y.H., 1998. Biotechnol. Prog. 14, 347–350.
Kedward, C.J., MacNaughtan, W., Blanshard, J.M.V., Blanshard, J.R., 1998. J. Food Sci. 63, 192–197.
Kedward, C.J., MacNaughtan, W., Mitchell, J.R., 2000a. J. Food Sci. 65, 324–328.
Kedward, C.J., MacNaughtan, W., Mitchell, J.R., 2000b. Carbohydr. Res. 329, 423–430.
Lai, H., Schmidt, S.J., 1990. J. Food Sci. 35, 994.
Mackin, L., Zanon, R., Park, J.M., Foster, K., Opalenik, H., Demonte, M., 2002. Int. J. Pharm. 231, 227–236.
Mahlin, D., Berggren, J., Alderborn, G., Engstrom, S., 2004. J. Pharm. Sci. 93, 29–37.
Mazzobre, M.F., Aguilera, J.M., Buera, M.P., 2003. Carbohydr. Res. 338, 541–548.
Opfermann, J., 2000. J. Therm. Anal. Cal. 60, 641–658.
Price, R., Young, P., 2004. J. Pharm. Sci. 93, 155–164.
Roos, Y.H., Karel, M., 1991. J. Food Sci. 56, 38–43.
Saleki-Gerhardt, A., Ahlneck, C., Zografi, G., 1994. Int. J. Pharm. 101, 237–247.
Schmitt, E.A., Law, D., Zhang, G.G.Z., 1999. J. Pharm. Sci. 88, 291–296.
Sebhatu, T., Alderborn, G., 1999. J. Pharm. Sci. 8, 235–242.
Takeuchi, H., Yasuki, T., Yamamoto, H., Kawashima, Y., 1999. Pharm. Dev. Technol. 4, 125–131.
Tzannis, S.T., Prestrelski, S.J., 1999. J. Pharm. Sci. 88, 360–370.
Vney, Y.D., Donhowe, D.P., Hartel, R.W., 1995. J. Food Sci. Technol. 30, 311–320.
Wade, A., Weller, P.J., 1994. Handbook of Pharmaceutical Excipients. Pharmaceutical Press, London.